Water Management
Volume 167 Issue WM3

Bottom outlet dam flow: physical and numerical modelling
Daneshmand, Adamowski and Liaghat

ice | proceedings

Proceedings of the Institution of Civil Engineers
Water Management 167 March 2014 Issue WM3
Pages 176–184 http://dx.doi.org/10.1680/wama.12.00048
Paper 1200048
Received 30/03/2012 Accepted 20/07/2012
Published online 27/03/2013
Keywords: dams, barrages & reservoirs/mathematical modelling/models (physical)

ice
Institution of Civil Engineers
publishing

Bottom outlet dam flow: physical and numerical modelling

Farhang Daneshmand PhD
Adjunct Associate Professor, Department of Bioresource Engineering, McGill University, Ste. Anne de Bellevue, Canada; Associate Professor, Faculty of Mechanical Engineering, Shiraz University, Shiraz, Iran

Jan Adamowski MPhil, MBA, PhD
Assistant Professor, Department of Bioresource Engineering, McGill University, Ste. Anne de Bellevue, Canada

Tahereh Liaghat MSc
Graduate Student, Mechanical Engineering Department, École Polytechnique de Montréal, Montréal, Canada

This paper presents an analysis of flow parameters through a bottom outlet conduit with gated operation using physical and numerical models. A physical model of the regulating bottom outlet of Shahryar dam in Iran was used to investigate the hydraulic forces on the service radial gate and flow patterns within the conduit. The model was constructed from Plexiglas, and discharge and pressure data were recorded for different gate openings. The Froude law of similarity was satisfied in the hydraulic modelling, allowing for an investigation of the dynamic similarity of inertial and gravitational forces. The numerical scheme was based on using the natural-element method to study hydraulic forces and flow parameters within the conduit and the finite-element method to evaluate the natural frequencies of the radial gate. The results of the calculations for different radial gate openings showed good agreement with those from physical modelling for the pressure distributions throughout the flow domain and on the gate.

1. Introduction

The Shahryar dam was constructed by the Iranian Ministry of Energy on the Ghezel-Owzan River (East Azerbaijan province in northwest Iran), 35 km from the city of Mianeh. Although the dam has been built, it is not yet in operation. The dam is designed to supply the required water for land downstream of the dam, 120 000 ha of Mianeh land and to provide the water required for agriculture and industry in Gilan province. Decreasing the amount of sediment entering the famous Sefid-rud dam downstream and providing 27 MWh of electricity annually are also aims for this dam (Nikbakhtan *et al.*, 2010). The Shahryar dam consists of a double-curvature arch dam of height 135 m and crest length 204 m. High flood discharges expected on the river are important, with Q_{1000} estimated at 5130 m^3/s, Q_{10000} at 8400 m^3/s and probable maximum flood at 14 570 m^3/s (when Q_{1000} and Q_{10000} are the inflow floods that occur at a return period of 1000 and 10 000 years, respectively). Dam and reservoir specifications are given in Table 1.

Dam height: m	135
Crest length: m	207
Crest elevation: m	1045
Mass and structural concrete: m^3	577 000
Open air and underground excavation: m^3	725 000
Embankment: m^3	3 925 000
Drilling and grouting: m	42 200
Tunnelling: m	3840
Bottom outlet sill elevation: m	1004
Total storage (at normal water level): million m^3	700
Normal water level: m	1035
Maximum water level: m	1041

Table 1. Specifications of the concrete double-arch Shahryar dam

The bottom outlet of the dam is equipped with a maintenance intake gate, a service gate and an emergency gate. The specifications of the gates are presented in Table 2. The maintenance gate is used for maintenance work on downstream equipment, such as gates and steel lining, and is operated in a fully opened or fully closed condition in balanced pressure. The balance pressure is attained by means of a bypass valve in the gate leaf. The gate is operated on a railway with a 12° inclination angle from the dam crest. Mathematical analyses and experience do not necessarily provide sufficient information to assure satisfactory performance and safety of the emergency and service gates. Therefore, model studies are often made to ensure cavitation- and vibration-free operation of the gates when they are put into service (USBR, 1980). The results of hydraulic model testing of the bottom outlet of the Shahryar dam are presented in this paper.

Fluid flow under sluice and radial gates has attracted considerable attention in the field of fluid mechanics due to its wide application in regulating the flow of water over spillway crests and through canals and other hydraulic structures. Flows under hydraulic gates have been considered as rapidly converging flows in which the influence of fluid viscosity is quite small compared with inertia effects and, consequently, the flow can be considered as irrotational. The basic difficulty in dealing with hydrodynamic free-surface flow problems lies in the fact that the unknown free

Maintenance gate (fixed wheel gate)	
Dimensions (width × height): m	3·85 × 6·2
Bed elevation: m	1005·75
Service gate (submerged radial gate)	
Discharge capacity at normal water level: m^3/s	250
Radius: m	5·2
Width: m	3·8
Opening (width × height): m	3 × 4
Manoeuvring speed: m/min	0·3
Seal type	Rubber seal
Emergency gate (high-pressure enclosed roller gate)	
Discharge capacity at normal water level: m^3/s	250
Gate dimensions (width × height): m	3·94 × 4·59
Opening dimensions (width × height): m	3 × 4·2
Manoeuvring speed: m/min	0·3
Seal type	Double-stem rubber seal

Table 2. Gate specifications (Daneshmand *et al.*, 2010)

surface is no longer a boundary of constant speed, due to the effect of gravity. Thus, application of Bernoulli's equation along the free surface leads to a non-linear coupling relationship (Abd-el-Malek, 1987, 1988; Abdel-Malek *et al.*, 1989). Among various numerical solutions to free-surface flows, the finite-element method (FEM) and boundary-element method have gained popularity in solving the free-surface problem (Daneshmand *et al.*, 2000). Use of finite-element analysis began with McCorquodale and Li (1971), who considered flow under a sluice gate. Many other studies have since appeared in the literature, including those reported by Bhajantri *et al.* (2007a, 2007b), Castro-Degado (1986), Chan *et al.* (1973), Chanel and Doering (2008), Daneshmand and Kazemzadeh-Parsi (2004), Guayjarernpanishk and Asavanant (2009), Helmi and El-Gamal (2011), Ikegawa and Washizu (1973), Li *et al.* (1989), Petrila (2002), Sankaranarayanan and Rao (1996) and Vanden-Broek (1997).

A computational scheme using a variable-domain and a fixed-domain natural-element method (NEM) can also be used for computation of the free-surface profiles, velocity and pressure distributions, and the flow rate of two-dimensional gravity fluid flow under emergency and radial gates. The fluid is assumed to be inviscid and incompressible in the numerical computations. The NEM is a Galerkin-based method that is built upon Voronoi diagrams and Delaunay tessellations (Cueto *et al.*, 2003; Daneshmand and Niroomandi, 2007; Sukumar *et al.*, 2001). This interpolation scheme has several very useful properties, such as its strictly interpolating character, its ability to exactly interpolate piecewise linear boundary conditions, and a well-defined and robust approximation with no user-defined parameter on non-uniform grids.

The dynamic behaviour and vibration characteristics of the radial service gate of the bottom outlet are also investigated in this paper. It is well known that gate vibration, when it occurs, can be a serious problem in many hydraulic projects (Kolkman and Jongeling, 2007). It can result in structural damage or may restrict operation of the gate at certain gate openings. In some cases, vibration of a gate will occur at specific hydraulic conditions that may only occur years after commissioning of the installation. Even when these have been identified, it may not be easy to reproduce them so that they can be investigated. There are various reasons for gate vibrations, such as excitation due to turbulence, excitation due to flow instability and self-excitation (excitation generated by the movement itself) (Naudascher and Rockwell, 1980).

2. Hydraulic model test

The aims of this test of the bottom outlet of the Shahryar dam included ascertaining gate discharge characteristics, gate loading, gate operations, pressure fluctuations, the absence of detrimental vibrations and the shape of water passages that do not include zones of low pressure with high cavitation potential. The experiments were carried out in the Department of Mechanical Engineering of Shiraz University in Iran.

2.1 Similarity criteria

A small-scale hydraulic model will reproduce the hydraulic phenomena of a prototype accurately if geometric and dynamic similarity between the prototype and its model is obtained. The similarity of hydrodynamics is the similarity of 'dynamic loads'. In order to ensure similarity of mean and fluctuation quantities, the Froude number (Fr), Reynolds number (Re), roughness and boundary conditions of the model and prototype need to be similar. Since it is impossible to ensure similarity of Fr and Re simultaneously, in practice, hydraulic models are usually scaled according to the Froude similarity. For Froude similarity, the fine-scale structure that is produced by viscous dissipation is not modelled. However, for a high Reynolds number, the energy dissipated by the fine scale of turbulence (which is produced by viscous dissipation) is much less than the total energy production. Therefore, for a high Reynolds number, a Froude model may accurately model the hydrodynamic loads produced by turbulence. For the bottom outlet of Shahryar dam and according to dam specifications, the Reynolds number in the channel is large enough ($71{\cdot}45 \times 10^6$) to ignore the energy dissipated by fine-scale turbulence. Hence, in the present hydraulic model test, the model for the gates and channel was constructed according to the Froude law. For a Froude model, the following scale relations are valid (Kolkman and Waterloopkundig, 1976)

1a. $$L_{\mathrm{m}} = L_{\mathrm{p}}/\lambda$$

1b. $$p_{\mathrm{m}} = p_{\mathrm{p}}/\lambda$$

1c. $$V_{\mathrm{m}} = V_{\mathrm{p}}/\lambda^{1/2}$$

1d. $$Q_{\mathrm{m}} = Q_{\mathrm{p}}/\lambda^{5/2}$$

1e. $$T_{\mathrm{m}} = T_{\mathrm{p}}/\lambda^{1/2}$$

where p is pressure, Q is volumetric flow rate, T is time, V is velocity, λ is the geometrical scale ($\lambda = 15$ in the present model) and m and p represent model and prototype, respectively.

3. Experimental setup and measurements

The hydraulic model test included the entire water passage, both upstream and downstream of the gate. The hydraulic model (scale 1:15) was constructed with Plexiglas to secure good flow visualisation and was operated with respect to Froude similarity (i.e. conserving the inertial and gravitational forces ratio). Water was provided from a pool, as shown in Figure 1 (upstream storage). The upstream storage is equipped with an adjustable weir to control the upstream water level. The test stand is depicted in Figure 2. The stand includes three centrifugal pumps,

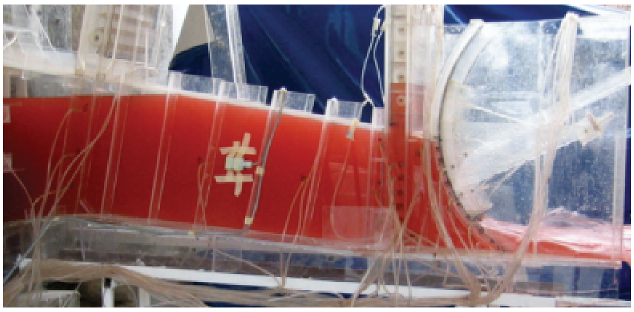

Figure 2. Experimental setup

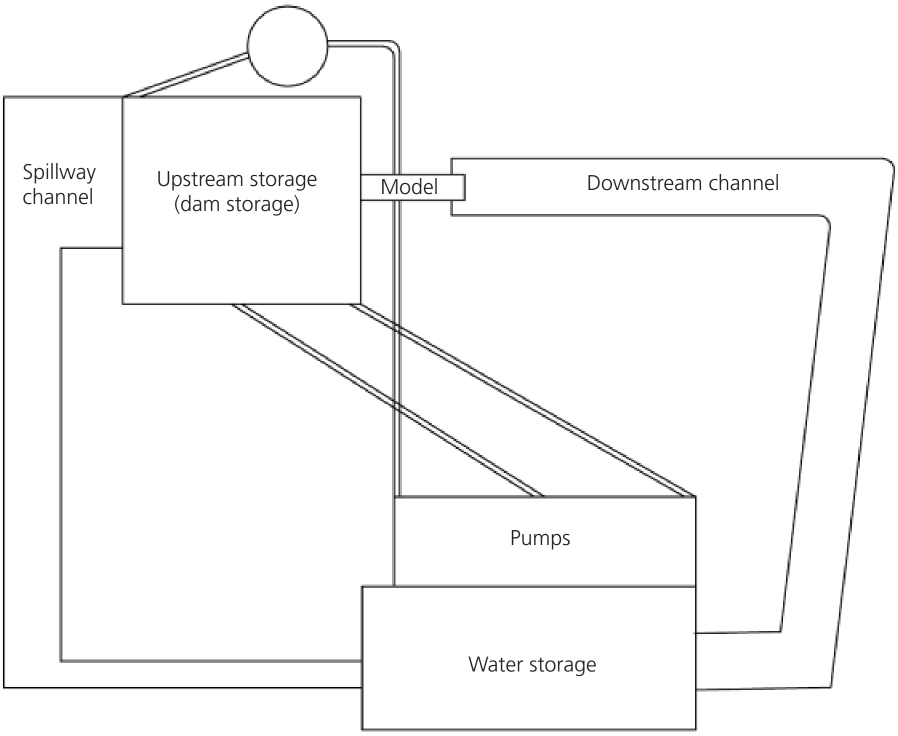

Figure 1. Sketch of the test stand

along with the main water storage and relevant channels to complete the closed-loop circuit.

3.1 Test procedure

Hydraulic tests were performed at gate openings of 2, 5, 10, 20, 30, 40, 50, 60, 70, 80, 90 and 100% of each gate and for the maximum water level of 1041 m. In each test, pressures at several locations in the channel, gate slots and on the skin plate of the gates were obtained by means of conventional manometers. The manometer locations are shown in Figure 3(a). The discharge characteristics of the radial gate were also measured at different radial gate openings and for elevations of 1006·0, 1011·8, 1017·6, 1023·4, 1029·2, 1035·0 and 1041·0 m. Water discharge was measured by using a rectangular weir placed downstream of the model; the measured values were also checked and confirmed using an area–velocity flow meter (Greyline AVFM-II). An ultrasonic sensor was installed at the bottom of the downstream channel. Based on the speed of sound in water, the level was measured with an accuracy of ±0·25%. Flow velocity was also measured, with an ultrasonic Doppler signal, to an accuracy of ±2%.

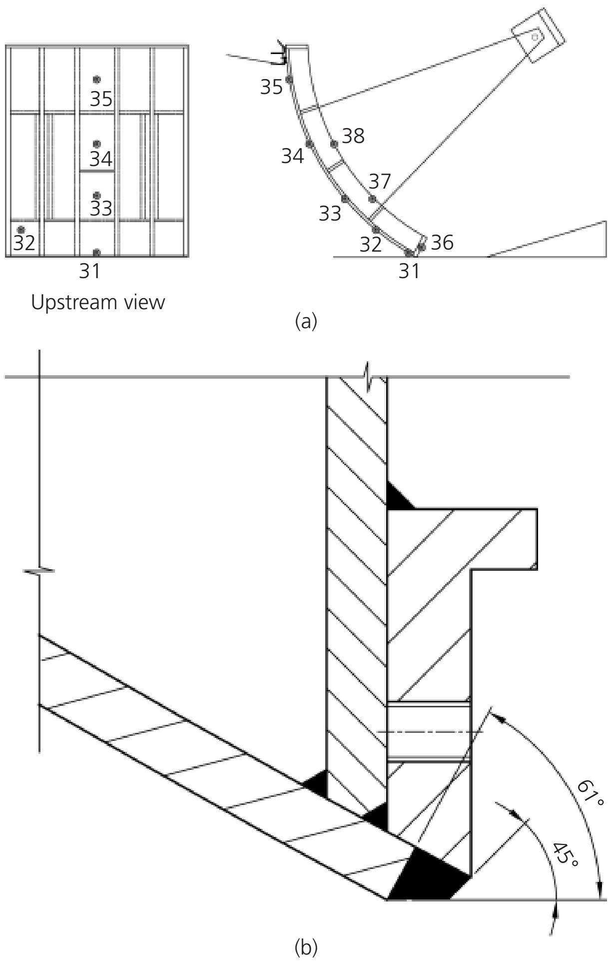

Figure 3. (a) Manometer locations on the service gate. (b) Gate lip of the service radial gate

3.2 Pressure fluctuations and fast Fourier transform (FFT) analysis

Due to turbulence, the local pressure p will fluctuate in a random fashion and can be expressed in terms of the average value $\bar{p}$ and fluctuating pressure p'. Hence (Naudascher, 1991)

$$2. \quad p = \bar{p} + p'$$

$$3. \quad \bar{p} = \lim_{T\to\infty} \frac{1}{T}\int_0^T p(t)\,\mathrm{d}t$$

$$4. \quad p'_{\mathrm{rms}} = (\bar{p'^2})^{1/2} \lim_{T\to\infty} \left[\frac{1}{T}\int_0^T p'^2(t)\,\mathrm{d}t\right]^{1/2}$$

Although p'_{rms} is usually sufficient to describe the magnitude of the pressures and forces, it gives no indication as to the rapidity of the variation in time. In other words, two flows could produce the same distributions of pressures with the same p'_{rms}, and yet one could be more rapidly fluctuating than the other. The power spectral density and FFT are used to describe the time aspect of pressures. The pressure fluctuations from the experiments were analysed by the FFT to obtain the power spectral densities of the fluctuation data. The frequency content of the pressure signal is also called 'the frequency spectrum'. The FFT algorithm greatly reduces the number of computations needed to convert the time signal into a frequency domain.

3.3 Numerical analysis

A computational scheme based on the NEM was also used to study the hydraulic forces and flow patterns developed within the conduit, and an FEM was used to find the natural frequencies of the radial service gate. The computational scheme based on the NEM uses a variable-domain and a fixed-domain NEM for computation of the free-surface profiles, velocity and pressure distributions and the flow rate of the fluid flow under the emergency and radial gates. The fluid is assumed to be inviscid and incompressible in the numerical computations. The detailed formulation and numerical algorithm have already been presented elsewhere (Daneshmand *et al.*, 2010). The numerical scheme was used to find the free-surface profiles of the flow under the emergency and radial service gates.

4. Data analysis and results

4.1 Pressure data

Pressure was measured at several locations in the channel and on the skin plate and stiffeners of the emergency and service gates. The pressure diagrams are shown in Figure 4 and Figure 5 for the service gate and emergency gate, respectively. The pressures measured were used to evaluate the cavitation index, hydrody-

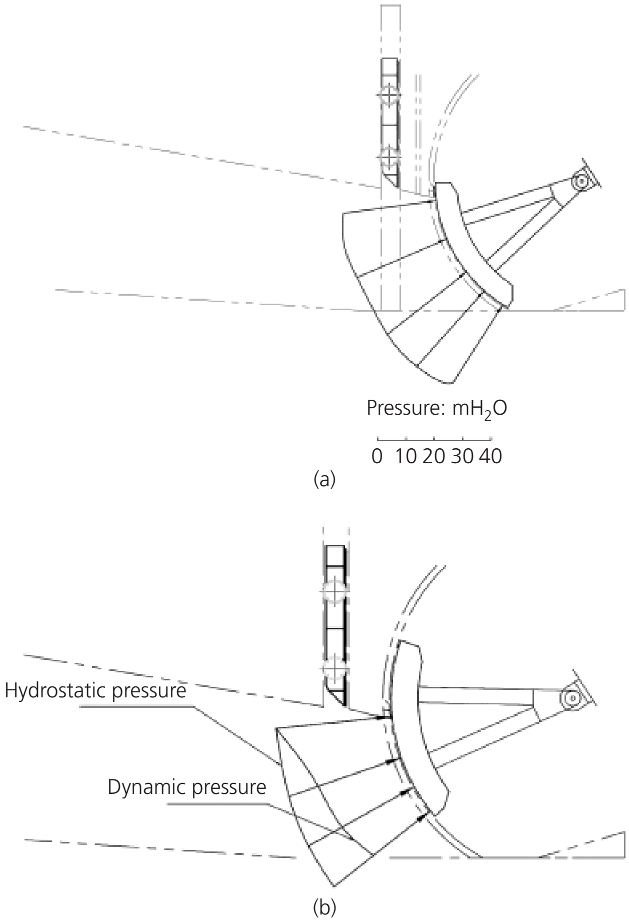

Figure 4. Pressures measured on the radial service gate: (a) 2% gate opening; (b) 30% gate opening

namic forces and aeration. Unsuitable design of the shape of the gate and tunnel may cause local negative pressures around the gate, which will induce cavitation damage to the gate and serious gate vibration. The results obtained in the model test indicated that all of the pressures were positive and so there was no low-pressure zone with high cavitation potential.

4.2 Discharge characteristics

Water discharge was measured using an area–velocity flow meter (Greyline AVFM-II). Its ultrasonic sensor was installed at the bottom of the downstream channel. A sharp-crested rectangular weir accompanied by a point gauge (for reading the height of water on the weir) was also used to measure the model discharge for small gate openings. The prototype discharges for the service gate openings from 2 to 100% at different elevations are shown in Figure 6. The discharge coefficients for the service gate at normal elevations were calculated according to

$$C_\mathrm{d} = \frac{Q}{A(2\boldsymbol{g}H)^{1/2}}$$

where Q is the discharge, A is the jet area, H is the head difference between the upstream and the centre of the jet and $\boldsymbol{g}$ is acceleration due to gravity. The discharge coefficient for the service gate at maximum elevation is given in Figure 7.

4.3 Hydrodynamic forces on gates

The hydrodynamic forces on the emergency gate for different openings at normal water level (= 1035 m) were calculated using (USBR, 1980)

5. $$\boldsymbol{F}_\mathrm{t} = \bar{P}_\mathrm{t} A_\mathrm{t}$$

6. $$\boldsymbol{F}_\mathrm{b} = \bar{P}_\mathrm{b} A_\mathrm{b}$$

7. $$\boldsymbol{F} = \boldsymbol{F}_\mathrm{t} - \boldsymbol{F}_\mathrm{b}$$

where $\boldsymbol{F}$ is the hydrodynamic force (down pull or up lift), $\bar{P}_\mathrm{t}$ is the average pressure on the top of the gate, $\bar{P}_\mathrm{b}$ is the average pressure on the bottom of the gate and A_t and A_b are projected area on the top and bottom of the gate, respectively. The results of this calculation are presented in Figure 8 for the emergency gate at different gate openings.

The force coefficients can also be calculated according to Equations 8–10 (Naudascher, 1991; USBR, 1980)

8. $$\boldsymbol{F} = \frac{(K_\mathrm{t} - K_\mathrm{b}) B d \rho V_\mathrm{c}^2}{2}$$

9. $$K_\mathrm{b} = \frac{2\boldsymbol{F}_\mathrm{b}}{\rho A_\mathrm{b} V_\mathrm{c}^2}$$

10. $$K_\mathrm{t} = \frac{P_\mathrm{t}}{\rho \boldsymbol{g} H}$$

where K_t and K_b are the force coefficients on the top and bottom of the gate, B is the width of the gate, d is the depth of the gate, $\boldsymbol{V}_\mathrm{c}$ is the velocity in the control section (using the measured discharge) and ρ is fluid density. Force coefficients are calculated and shown in Figure 9.

4.4 Pressure fluctuations and FFT analysis

Radial gates are the most frequently used movable water control structures and are most widely used as the crest control gates. They are particularly suitable because of their simplicity of design, construction and installation. Radial gates are used in conduits to control high-velocity flow. One desirable feature of a

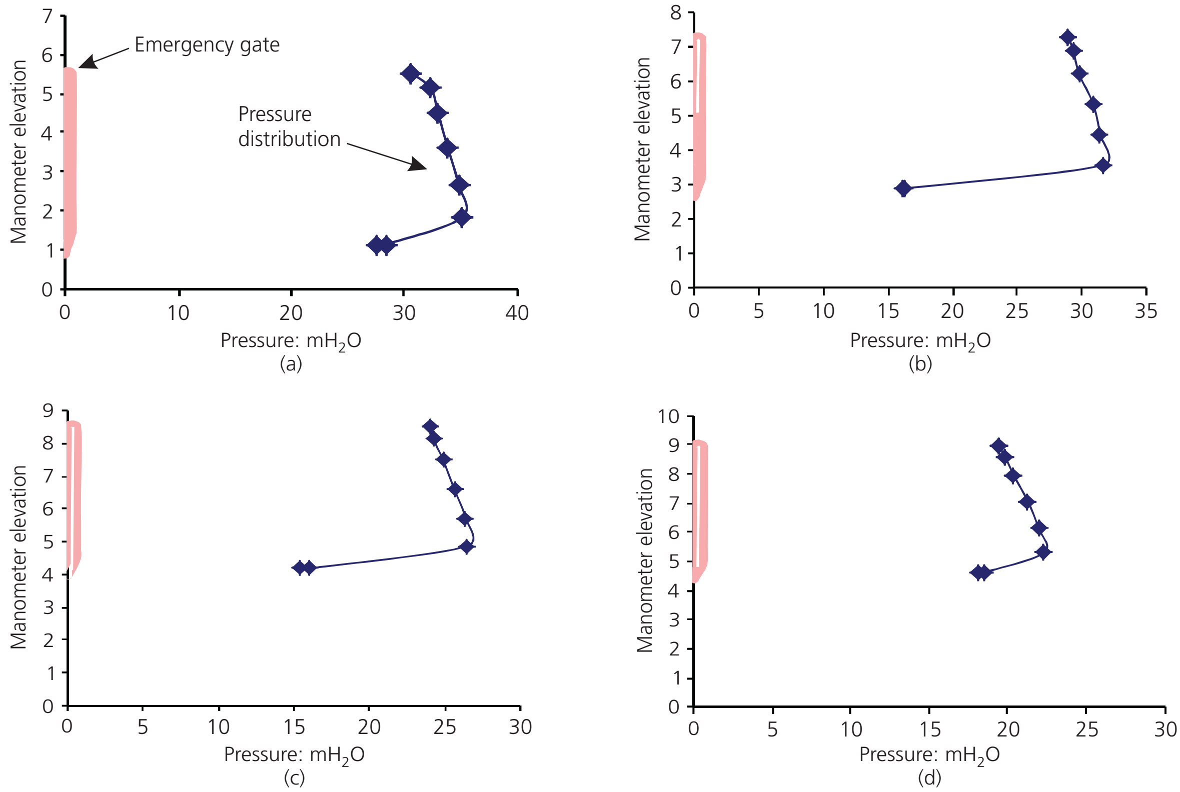

Figure 5. Pressures measured on the emergency gate for service gate opening of 100% and emergency gate openings of (a) 10%, (b) 50%, (c) 80% and (d) 90%

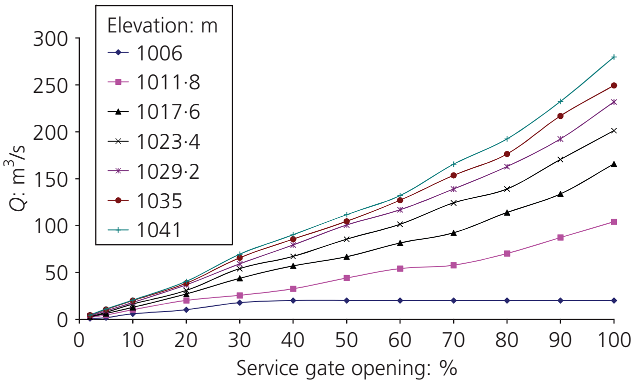

Figure 6. Prototype discharge for service gate openings

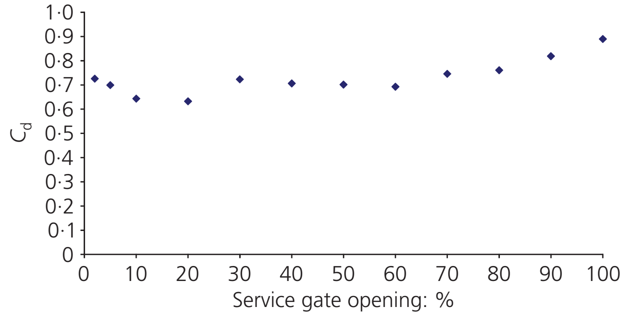

Figure 7. Prototype discharge coefficient for different service gate openings (normal water level)

radial gate is that it needs no gate slots. The opening of a radial gate requires less hoisting force, and such gates can thus be moved up or down more easily than other types of gates. This ability also makes this gate more sensitive to vibration, and more attention should be given to exploring the dynamic behaviour of the gate. In this work, the pressure fluctuations induced by turbulence on the skin plate at different local openings were measured and the dominant exciting frequencies extracted from FFT analysis. To avoid resonance, the natural frequencies of the service gate should be different from the exciting frequencies. The pressure fluctuating from the experiments should be analysed by the FFT to obtain the power spectral densities of the fluctuation data. The results of these calculations are shown in Figure 10 for radial service gate openings of 10 and 40%. It should be noted that the dynamic pressures of flow can be influenced by vibrations of the experimental setup; appropriate supports were used in the setup to prevent such vibrations as much as possible.

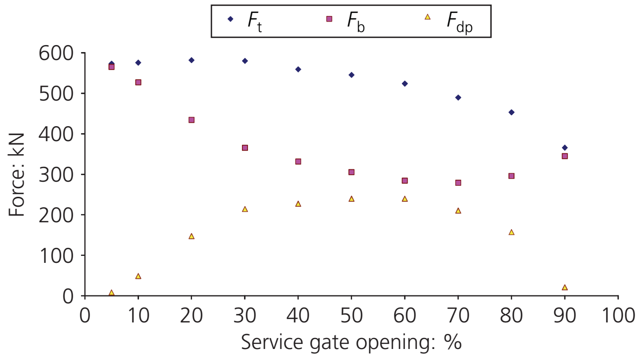

Figure 8. Hydrodynamic forces on the emergency gate. F_{dp}, downpull force

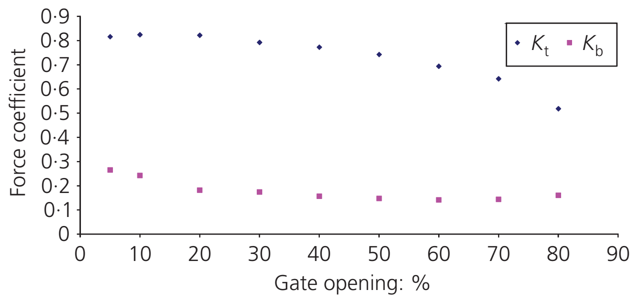

Figure 9. Hydrodynamic force coefficients for the service gate

Vibration of a radial gate can be directly due to fluctuating pressures on the gate, and it is thus important to obtain correct pressure fluctuation data for any evaluation of gate vibration. Graphs of the power spectrum densities and the root mean square of pressure fluctuations at each test point showed that the pressure fluctuations on the gate were not large under normal discharge of radial gate local openings. The FEM was also used to obtain the frequencies of the radial gate. Two different boundary conditions were considered in the numerical calculations. All nodes on the bottom of the skin plate were assumed to be free in the normal direction and fixed in the first and second boundary conditions. The first vibration frequencies of the service radial gate were calculated to be 2·09 Hz and 2·13 Hz for the first and second boundary conditions, respectively. These frequencies are sufficiently far away from the peaks in the power spectral densities shown in Figure 10.

As an appropriate approach to predict the behaviour of gravity-affected flow under a sluice gate with very high accuracy, the NEM was used to find the shape of free-surface flow under the sluice emergency and radial service gates. In both gates, a rapid rate of convergence was always observed, even with an initial guess that differed greatly from the true solution. The mathematical formulation and numerical details of the procedure are given elsewhere (Daneshmand *et al.*, 2010), and are not presented here for the sake of brevity. In spite of the non-linear nature of the problem, the numerical scheme as used in the present work did not need an excessive number of iterations, and the iteration procedure converged quite rapidly. The numerical results from the proposed method were in good agreement with those obtained from the hydraulic model test.

For the case of the radial service gate, the NEM was used with 855 nodes and 1328 elements (in the first iteration). The discretisation was made finer in the vicinity of the gate to account for the higher velocity gradients in that region. The result for the free-surface shape of the flow under the emergency sluice gate is shown in Figure 10 (Daneshmand *et al.*, 2010). Figure 11 shows the free-surface flow under the emergency gate. The velocity contour of the flow under the radial service gate for a 30% opening is shown in Figure 12 (Daneshmand *et al.*, 2012).

Certain undesirable hydraulic conditions, such as hydraulic jumps and submerged bottoms, may still induce serious gate vibrations. When the vibration sources formed by such hydraulic conditions vanish, vibration of the gate will disappear. As such, the best way

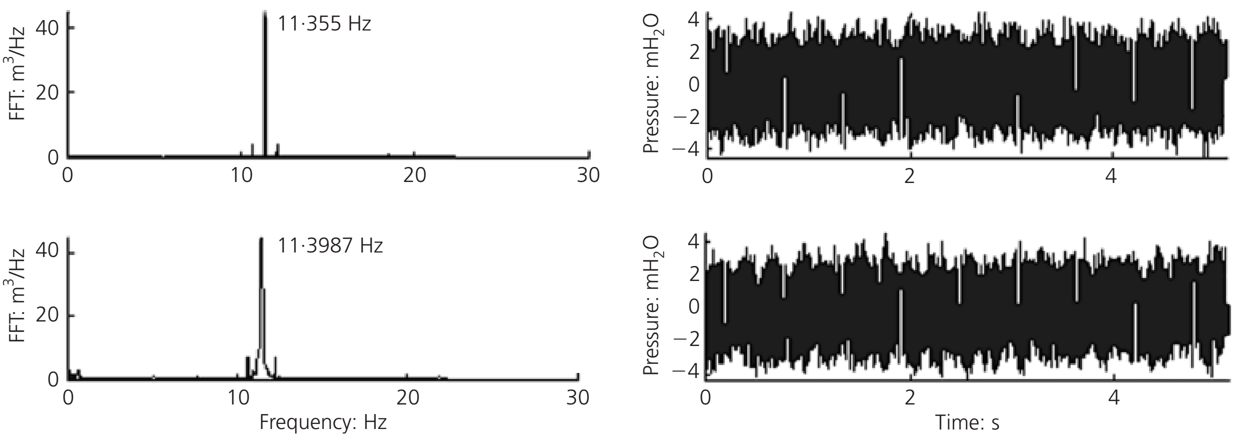

Figure 10. Power spectral densities and pressure fluctuations for 10% and 40% service gate openings

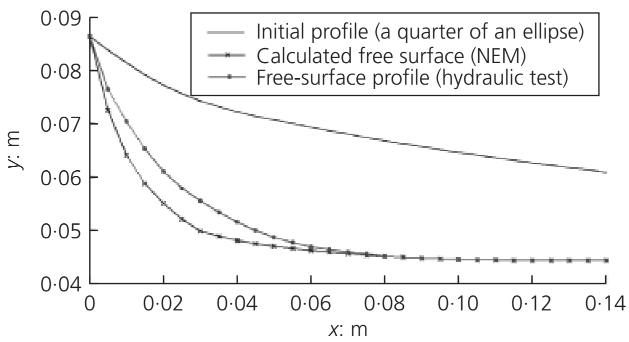

Figure 11. Free-surface profile of the flow under the emergency sluice gate (Daneshmand *et al.*, 2010)

to prevent this type of vibration is to eliminate the sources of vibration. By observing the shapes of water passage, both in the liner and under the gate, no undesirable feature was observed. It was concluded that the sources of this type of vibration were properly eliminated and vibration could not be induced in the gate by these sources.

5. Conclusions

With rapidly changing advances in numerical modelling, engineers now face the possibility of using combined physical and computational methods in the design and analysis of hydraulic structures and conduits. A combined physical and numerical method was presented in this paper. The physical model was based on the Froude similarity criteria, whereas the numerical analysis was performed using NEMs and FEMs. The results of a hydraulic model test of the bottom outlet of Shahryar dam in Iran were presented. The main results of the hydraulic test were gate discharge characteristics, gate loading and the shape of water passage, which did not include zones of low pressure with high cavitation potential. The measured values of pressure were used to evaluate the hydrodynamic forces and force coefficients. A computational procedure based on the NEM was used to predict the free-surface profile of the flow under the emergency gate and the velocity contour in the channel. The dynamic characteristics of the radial gate of Shahryar dam were studied in the hydraulic model test. Pressure fluctuations induced by turbulence on the skin plate at different local openings, which is the basic dynamic load acting on the gates, were also investigated. The FEM was also used to analyse the free vibration characteristics of the radial gate at different openings. The measurements showed that the pressure fluctuations in the present case were random in the time domain. Moreover, the results obtained from the hydraulic model test showed that the fundamental frequency of the service radial gate was sufficiently far from the dominant frequencies in the power spectral density of the pressure fluctuations and therefore the gate is free from the risk of resonance. There was reasonably good agreement between the physical and numerical models.

Acknowledgements

The authors would like to thank K. Azodi Ghajar and M. Chahabkari for their assistance in constructing the hydraulic model and taking part in various measurements. An NSERC Discovery Grant held by Jan Adamowski was used to partially fund this research.

REFERENCES

Abd-el-Malek MB (1987) Approximate solution for gravity flow under a sluice gate. *Journal of Computational and Applied Mathematics* **35(1–3)**: 83–97.

Abd-el-Malek MB (1988) Local behaviour of an inviscid flow from a uniform channel over a sharp-crested weir. *Acta Mechanica* **72(3–4)**: 233–244.

Abdel-Malek MN, Hanna SN and Abd-el-Malek MB (1989) Approximate solution for gravity flow under a Tainter gate. *Journal of Computational and Applied Mathematics* **26(3)**: 271–279.

Bhajantri MR, Eldho TI and Deolalikar PB (2007a) Modeling hydrodynamic flow over spillway using weakly compressible flow equations. *Journal of Hydraulic Research* **45(6)**: 844–852.

Bhajantri MR, Eldho TI and Deolalikar PB (2007b) Numerical modelling of turbulent flow through spillway with gated

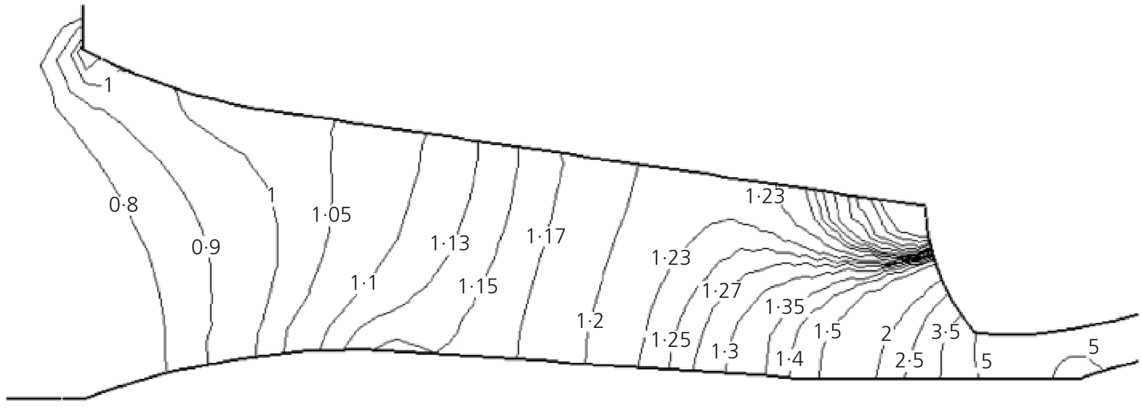

Figure 12. Velocity contour for a radial gate opening of 30%

operation. *International Journal for Numerical Methods in Engineering* **72(2)**: 221–243.

Castro-Degado M (1986) Analysis of free-surface flows past overflow gates using finite element method. *Computers and Fluids* **14(2)**: 159–169.

Chan STK, Larock BE and Herrmann LR (1973) Free-surface ideal fluid flows by finite elements. *Journal of the Hydraulic Division ASCE* **99(6)**: 959–974.

Chanel PG and Doering JC (2008) Assessment of spillway modeling using computational fluid dynamics. *Canadian Journal of Civil Engineering* **35(12)**: 1481–1485.

Cueto E, Sukumar N, Calvo B *et al.* (2003) Overview and recent advances in natural neighbour Galerkin methods. *Archives of Computational Methods in Engineering* **10(4)**: 307–384.

Daneshmand F and Kazemzadeh-Parsi MJ (2004) A meshless method for free surface flow through sluice gates. In *Proceedings of 6th International Conference on Hydroinformatics* (Liong S-Y, Phoon K-K and Babovic V (eds.)). World Scientific Publishing, Singapore, 71–78.

Daneshmand F and Niroomandi S (2007) Natural neighbour Galerkin computation of the vibration modes of fluid–structure systems. *Engineering Computations* **24(3)**: 269–287.

Daneshmand F, Sharan SK and Kadivar MH (2000) Finite-element analysis of double-free-surface flow through slit in dam. *Journal of Engineering Mechanics* **126(5)**: 515–522.

Daneshmand F, Javanmard SAS, Liaghat T, Moshksar MM and Adamowski JF (2010) Numerical solution for two-dimensional flow under sluice gates using the natural element method. *Canadian Journal of Civil Engineering* **37(12)**: 1550–1559.

Daneshmand F, Javanmard SAS, Adamowski JF, Liaghat T and Moshksar MM (2012) Two-dimensional natural element analysis of double-free surface flow under a radial gate. *Canadian Journal of Civil Engineering* **39**: 643–653.

Guayjarernpanishk P and Asavanant J (2009) Numerical solutions of flows under an inclined gate. *Thai Journal of Mathematics* **7(1)**: 171–187.

Helmi AM and El-Gamal MH (2011) Experimental and numerical investigations of flow through free double baffled gates. *Water SA* **37(2)**: 245–254.

Ikegawa M and Washizu K (1973) Finite element method applied to analysis of flow over a spillway crest. *International Journal for Numerical Methods in Engineering* **6(2)**: 179–189.

Kolkman PA and Jongeling THG (2007) *Dynamic Behaviour of Hydraulic Structures*. Delft University of Technology, Delft, The Netherlands.

Kolkman PA and Waterloopkundig L (1976) *Flow-induced Gate Vibrations: Prevention of Self-excitation: Computation of Dynamic Gate Behaviour and the Use of Models*. Delft Hydraulics Laboratory, Delft, The Netherlands.

Li W, Xie Q and Chen CJ (1989) Finite analytic solution of flow over spillways. *Journal of Engineering Mechanics ASCE* **150(12)**: 2635–2648.

McCorquodale JA and Li CY (1971) Finite element analysis of sluice gate flow. *Transactions of the Engineering Institute of Canada*. Engineering Institute of Canada, Montreal, Canada, vol. 14.

Naudascher E (1991) *Hydrodynamic Forces*. Taylor & Francis, Balkema, Rotterdam, The Netherlands.

Naudascher E and Rockwell D (1980) Oscillator-model approach to the identification and assessment of flow-induced vibrations in a system. *Journal of Hydraulic Research* **18(1)**: 59–82.

Nikbakhtan B, Ahangari K and Rahmani N (2010) Estimation of jet grouting parameters in Shahriar dam, Iran. *Mining Science and Technology (China)* **20(3)**: 472–477.

Petrila T (2002) Mathematical model for the free surface flow under a sluice gate. *Applied Mathematics and Computation* **125(1)**: 49–58.

Sankaranarayanan S and Rao HS (1996) Finite element analysis of free surface flow through gates. *International Journal for Numerical Methods in Fluids* **22(5)**: 375–392.

Sukumar N, Moran B, Semenov AY and Belikov VV (2001) Natural neighbour Galerkin methods. *International Journal for Numerical Methods in Engineering* **50(1)**: 1–27.

USBR (United States Bureau of Reclamation) (1980) *Hydraulic Laboratory Techniques*. USBR, Denver, CO, USA.

Vanden-Broek JM (1997) Numerical calculations of the free surface flow under a sluice gate. *Journal of Fluid Mechanics* **330**: 339–347.